Highly efficient and stable Ru nanoparticle electrocatalyst for the hydrogen evolution reaction in alkaline conditions

Frederik Søndergaard-Pedersen,[a] Harish Lakhotiya,[a] Martin Bondesgaard,[a] Munkhshur Myekhlai,[b] Tania M. Benedetti,[b] J. Justin Gooding,[b,c] Richard D. Tilley,*[b,c,d] and Bo B. Iversen*[a]

[a] Center for Materials Crystallography, Department of Chemistry and iNANO, Aarhus University, DK8000 Aarhus C (Denmark). [b] School of Chemistry, University of New South Wales, Sydney, New South Wales 2052 (Australia). [c] Electron Microscope Unit, Mark Wainwright Analytical Centre, University of New South Wales, Sydney, New South Wales 2052 (Australia). [d] Australian Research Council Centre of Excellence in Convergent Bio-Nano Science and Technology, University of New South Wales, Sydney, New South Wales 2052 (Australia).

Corresponding authors: r.tilley@unsw.edu.au or bo@chem.au.dk

Abstract: Developing alternatives to platinum-based electrocatalysts for the hydrogen evolution reaction (HER) is an important challenge for realizing the green transition. This is especially the case for alkaline conditions where Pt-based catalysts have very poor stability. Here, we demonstrate new solvothermal synthesis methods with facile allotropism control for selectively obtaining hexagonal-close-packed (hcp) and face-centered cubic (fcc) ruthenium nanoparticles. Both samples are highly active HER catalysts in alkaline conditions outperforming commercial Pt/C. However, the samples show markedly different stabilities. The hcp sample shows exceptional stability for 12 hours constant operation at 10 mA/cm^2 with an overpotential that only increases 6 mV whereas the fcc sample increases 50 mV and the commercial Pt/C more than 350 mV. Thus, this study underlines the importance of controlling the crystal structure of nanoparticle electrocatalysts and shows the potential of using Ru as an alternative to Pt in alkaline conditions.

Production of hydrogen via electrochemical water splitting is expected to be a central technology in order to achieve a society that runs entirely on renewable energy.[1] This will enable both storage of intermittent energy sources such as wind and solar as well as decarbonization of heavy-duty transport (e.g. trucks, ships and airplanes) that cannot be electrified easily. Today, alkaline electrolysis is the most mature electrolysis technology, however, the hydrogen evolution reaction (HER) occurring at the cathode in alkaline conditions is still two to three orders of magnitude slower than in acidic solutions.[2] Pt is the most active HER catalyst, but it is scarce and expensive, which prevents its large-scale commercial use.[3] Furthermore, Pt shows very poor durability in alkaline HER conditions. These issues have generated interest for finding Pt-free but equally active HER catalysts.[4]

In recent years, Ru nanoparticles have emerged as a potential substitute for Pt as HER catalyst, where a very high surface-to-volume ratio maximizes the number of available active sites.[5] Ru is significantly

cheaper than Pt and stable in both acidic and alkaline conditions making it a versatile HER catalyst.[6] In alkaline conditions, geometric current densities of 10 mA/cm^2 have previously been achieved at low overpotentials in the range of 5-95 mV and with low Tafel slopes of 30-70 mV/dec.[5, 7] Ru nanoparticles have been synthesized using a multitude of methods[5] including thermal decomposition/pyrolysis,[8] electroreduction,[9] solution/organometallic methods[7d, 10] and even room temperature solid-state synthesis.[7a] Solvothermal synthesis is a green alternative for the preparation of nanomaterials ranging from simple metals and metal oxides to highly complex solid solutions.[11] It is a fast and easy single-step method that can be performed using simple equipment making it highly suitable for upscaling. The obvious versatility of solvothermal synthetic methods is complemented by the precise control over polymorphism, crystallinity, size and shape distributions via simple synthesis parameters such as temperature, time of reaction, choice of solvent, precursor and potential surfactants the method provides.[11a]

For Ru nanoparticles, it has been shown that the allotropism can be controlled by using the ruthenium(III) acetylacetonate precursor (Ru(acac)$_3$) in solvothermal synthesis with absolute ethanol as solvent as it yields the typically adopted hexagonal close packed (hcp) structure at high temperature whereas the unusual face-centered cubic (fcc) structure can be obtained at low temperature.[12] Previously, Ru nanoparticles with the fcc structure have shown to be attractive for catalyzing CO oxidation and alkaline hydrogen oxidation.[13] Reports have also indicated that the presence of Ru with the fcc structure either as mixed-phase or phase-pure particles is beneficial for the catalytic HER performance in alkaline conditions.[14] Ru nanoparticles with the hcp structure have been shown to be promising catalysts for hydrogenation reactions as well as for the oxygen evolution reaction in acidic conditions.[10a, 15] Here, we report new facile solvothermal syntheses of ultrasmall hcp and fcc Ru nanoparticles with allotropism control simply via the choice of solvent. The small particles are obtained without the need of any surfactant or capping agent and this is attractive for catalytic applications due to the high specific surface areas that can be achieved.[5] Both the hcp and fcc samples are active HER catalysts in alkaline conditions, but the hcp Ru sample shows exceptional stability with a low overpotential of 46 mV to reach 10 mA/cm^2, which only increases 6 mV after 12 hours of constant operation. This is significantly better than the increases observed for fcc Ru (50 mV) and commercial reference catalysts (59 mV for Ru/C and 353 mV for Pt/C), which thus show significant losses of activity. This shows the potential of the easily scalable solvothermal method for producing very active and stable nanoparticle electrocatalysts.

Solvothermal synthesis was used to produce small metallic Ru nanoparticles with control of the allotropism via the choice of solvent. Ruthenium(III) acetylacetonate (Ru(acac)$_3$) was used as Ru precursor in the autoclave syntheses with water or a mixture of acetone and ethanol as solvents (see detailed experimental procedure in the supporting information, SI). Powder X-ray diffraction (PXRD) patterns show that the sample

prepared with water as solvent has the conventional hcp structure whereas the non-conventional fcc structure was obtained when 50:50 V% ethanol/acetone was employed as the solvent (Fig. 1a and 1d). It has been suggested previously that the $Ru(acac)_3$ precursor is important for stabilizing fcc Ru in triethylene glycol or at low temperature in ethanol due to strong coordination of the acetylacetonate anion and stabilization of the {111} facet.[12, 16] However, this does not occur when water is used as the solvent possibly due to the lower miscibility of acetylacetonate.

The broad peaks observed in the diffraction patterns of both samples indicate the presence of ultrasmall crystallite sizes of the nanoparticles. This is further confirmed from transmission electron microscopy (TEM) images (Fig. 1, S1 and S2). The TEM images show the presence of both monodisperse small primary particles of a few nanometers and their agglomerations. Rietveld refinements of the diffraction patterns yield volume-averaged crystallite domain sizes of 3.3(2) nm for the Ru hcp sample whereas it is 1.0(3) nm for the Ru fcc sample (see details on refinement procedures and extracted values in SI, table S1). Elemental mapping via scanning transmission electron microscopy-energy dispersive X-ray spectroscopy (STEM-EDS) shows the distribution of ruthenium in the samples, and also shows the presence of some oxygen in both samples (see Fig. S3-S6).

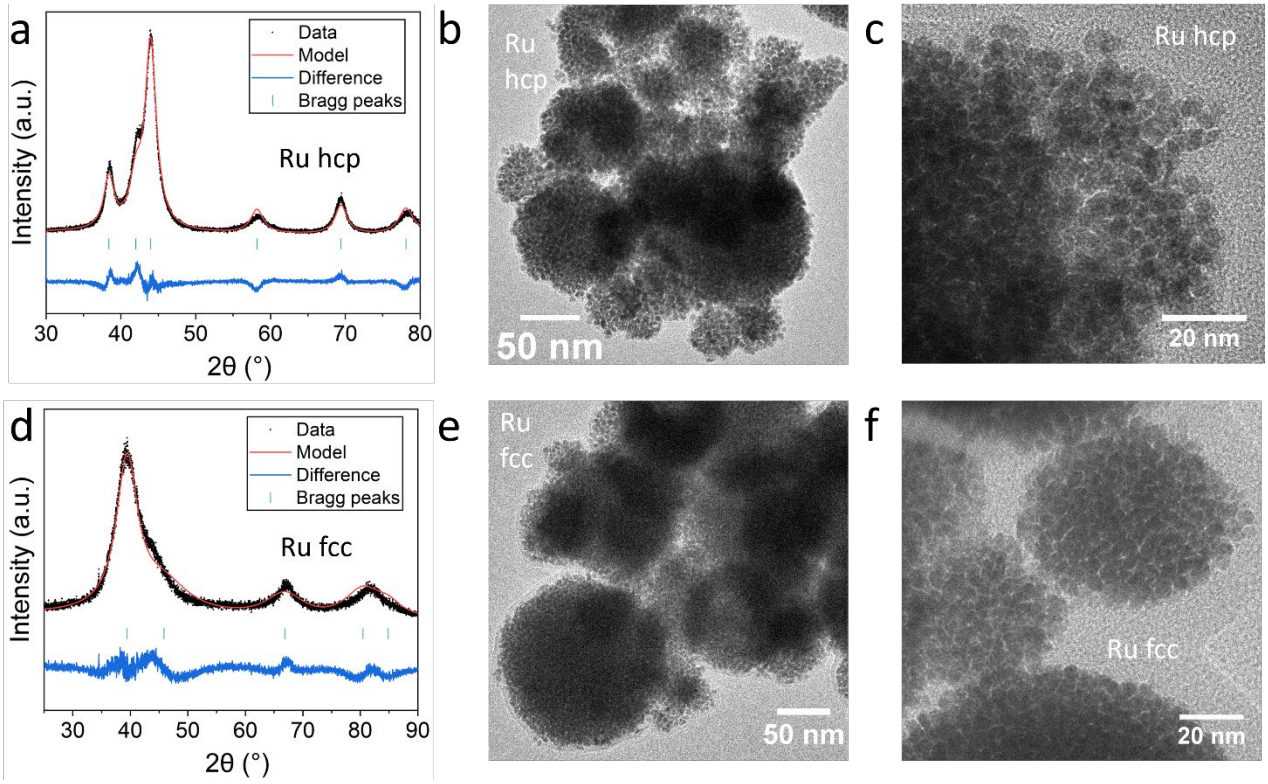

Fig. 1. Characterizations of the Ru hcp (a, b, c) and Ru fcc samples (d, e, f) by PXRD and Rietveld refinement and bright field TEM images.

The Ru hcp and fcc catalysts were tested for the HER reaction in 1.0 M NaOH (see experimental details in SI). A testing protocol inspired by McCrory *et al.*[17] (Fig. S7) was used to measure the activity of the samples before and after the stability test on the same films as well as to ensure similar testing conditions for all samples. Both samples present high activity for HER catalysis in the strong alkaline conditions reaching 10 mA/cm^2 at a low overpotentials of 46 mV for the Ru hcp and 54 mV for the Ru fcc (Fig. 2a). Thus, the Ru hcp sample is the most active, and the activity difference becomes even more pronounced at higher current densities (it requires only 57 mV overpotential to reach 19.5 mA/cm^2). This is comparable to previous reports on Ru-based HER catalysts (see Table S2).[5] For comparison, two commercial catalysts were also tested under the same conditions: 40 wt% Ru/C and 20 wt% Pt/C (see details in SI). The commercial Ru/C catalyst contains Ru nanoparticles with the hcp structure and estimated crystallite size around 3 nm that is similar to the catalysts obtained by the solvothermal method (Fig. S8 and S9). The commercial sample requires an overpotential of 51 mV to reach 10 mA/cm^2 current density, which is only 5 mV higher than our best performing sample. However, the required overpotential gap increases dramatically at the higher current density *i.e.* 70 mV to reach 19.5 mA/cm^2, which is 13 mV higher and tends to increase more (Fig. 2a). The commercial Pt/C sample is considerably less active requiring an overpotential of 110 mV to reach 10 mA/cm^2 displaying the superiority of Ru-based HER catalysts in strongly alkaline conditions.

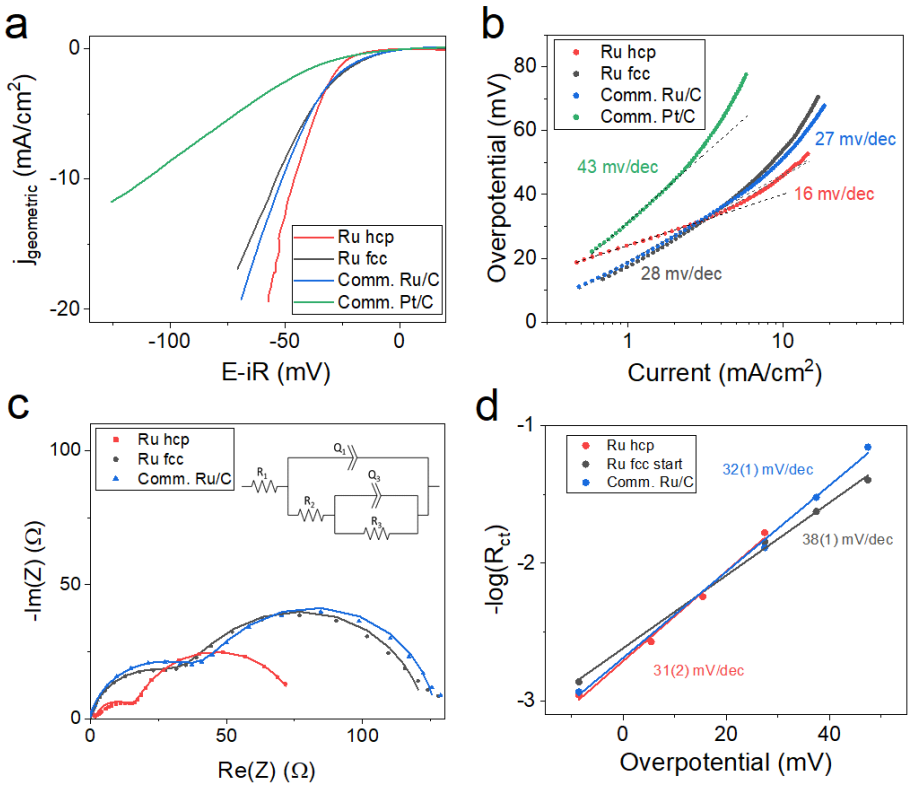

Fig. 2. HER activity assessment in 1.0 M NaOH. a) iR-corrected linear scan voltammograms showing the geometric current density. b) Tafel plot. c) Nyquist plots of the obtained EIS spectra (dots) obtained at an overpotential of 27 mV and

fit results (solid lines) from the equivalent circuit model shown in the inset. d) Plot of the charge transfer resistance versus overpotential.

The Tafel slope of the Ru hcp sample is found to be very low at only 16 mV/dec (Fig. 2b). The other samples show higher Tafel slopes of 27 mV/dec for the Ru fcc sample, 28 mV/dec for the commercial Ru/C samples and 43 mV/dec for the commercial Pt/C sample.

The intrinsic activities of all samples for the HER reactions were analysed by performing electrochemical impedance spectroscopy (EIS) at a range of different overpotentials (see Fig. 2c and S10). All the EIS spectra feature two semi-circles in the Nyquist plot. The semi-circle at higher frequency does not change with increasing overpotential whereas the resistance of the lower frequency semi-circle decreases with increasing overpotential so this is interpreted as representing the HER reaction (see Fig. S10). All the EIS spectra were fitted using the equivalent circuit model shown in the inset of Fig. 2c (see results in table S3). At an overpotential of 27 mV, the Ru fcc and commercial Ru/C samples show charge transfer resistances, R_{ct}, of 70 and 77 Ω, respectively, whereas the Ru hcp sample has an R_{ct} of only 60 Ω at the same overpotential. This indicates that the Ru hcp sample has a higher intrinsic activity for the HER reaction which results in the higher current response observed in the LSVs compared to the other samples. The charge transfer resistances decrease with increasing overpotential and this dependence can be used to determine Tafel slopes.[18] Plots of $-\log(R_{ct})$ versus overpotential yield straight lines that were linear fitted and Tafel slopes were determined as the reciprocal of their slopes (Fig. 2d).[19] The resulting values of the Tafel slopes obtained in this way are slightly higher than the values obtained from the Tafel plots obtained via voltammetry. However, Tafel slopes from EIS have been reported to be more accurate as they purely reflect the charge transfer kinetics whereas those from voltammetry may include contributions from catalyst resistance.[18] Thus, the EIS Tafel slopes for Ru hcp (31(2) mV/dec) and commercial Ru/C (32(1) mV/dec) indicate that their rate-determining step is the Tafel step, which has a characteristic Tafel slope of 30 mV/dec.[5, 20] This is in contrast to the Heyrovsky step with a characteristic Tafel slope of 40 mV/dec, which seems to be rate-determining for the Ru fcc sample.

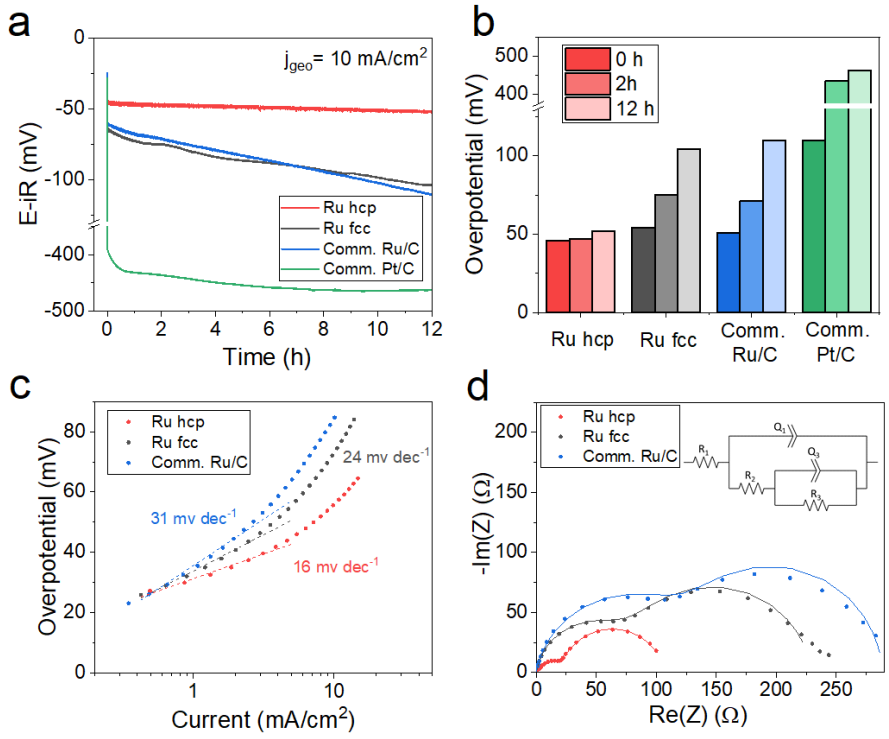

Fig. 3. HER stability tests. a) Stability tests by performing chronopotentiometry at 10 mA/cm^2 for 12 hours. b) Overpotentials required for 10 mA/cm^2 current density from the chronopotentiometry measurements after 0, 2 and 12 hours. c) Tafel plots obtained after the 12 hour stability tests. d) Nyquist plots of the obtained EIS spectra after 12 hour stability tests (dots) obtained at an overpotential of 27 mV and fitting results (solid lines) from the equivalent circuit model shown in the inset.

The stability of the samples was assessed by performing chronopotentiometry for 12 hours at a constant current density of 10 mA/cm^2 (Fig. 3a). The Ru hcp sample shows excellent stability as the required overpotential is nearly constant with an increase of only 6 mV after 12 hours (Fig. 3b). In contrast, the activities of the Ru fcc and commercial Ru/C catalysts decrease at constant and nearly equal rates, which result in overpotentials that have increased 50 mv for Ru fcc and 59 mV for commercial Ru/C after 12 hours. The commercial Pt/C sample shows an overpotential at 10 mA/cm^2 that increases rapidly to more than 400 mV exemplifying the stability issues when using Pt-based HER catalysts in strong alkaline conditions. The observed deactivation of the Ru fcc sample is in contrast to previous reports, which have showed relatively high stabilities in chronoamperometry tests for 2-50 hours.[14] However, in those studies the fcc Ru particles have either been supported on graphitic C_3N_4 on carbon or they form part of inter-grown Ru hcp and fcc nanodendrites, which may improve the stability relative to the unsupported phase-pure fcc nanoparticles presented in this study.

The Ru hcp sample retains a Tafel slope of only 16 mV/dec after the 12 hour chronopotentiometry test (Fig. 3c) indicating that the reaction kinetic remains similar to before the stability test. The Ru fcc and commercial

Ru/C samples still have higher Tafel slopes at 24 and 31 mV/dec, respectively. ECSAs were determined again after the chronopotentiometry tests and showed a negligible decrease (Table S3).

EIS spectra were also obtained after the 12 h stability tests (Figure 3d). Here, the diameter of the low-frequency semi-circle has increased significantly for Ru fcc and commercial Ru/C, whereas it only has increased marginally for Ru hcp. This further corroborates the chronopotentiometry results and the exceptional stability of the Ru hcp catalyst. The fitted values of the charge transfer resistance is now 81 Ω for the Ru hcp sample (up from 60 Ω before chronopotentiometry test), but it has increased to 137 and 135 Ω for the Ru fcc and commercial Ru/C samples, respectively, which are nearly double of their initial values. This shows that the Ru hcp sample retains a high intrinsic activity whereas those of the Ru fcc and commercial Ru/C samples degrade significantly. This could possibly be due to higher crystallinity or the presence of more favourable faceting in the Ru hcp sample.

In conclusion, we demonstrate new solvothermal synthetic protocols with facile control over the fcc and hcp structures of Ru to produce highly active and stable nanoparticle electrocatalysts for the HER reaction under highly attractive but demanding alkaline conditions. The prepared Ru hcp catalyst shows exceptional stability with an overpotential at 10 mA/cm^2 that only increases 6 mV during 12 hour chronopotentiometry testing. This significantly outperforms both the prepared Ru fcc catalyst, which increases 50 mV as well as the commercial Ru/C and Pt/C reference catalysts, which increase 59 and 353 mV, respectively. Thus, the study shows the potential of using Ru-based electrocatalysts as an alternative to Pt in alkaline conditions.

Acknowledgements

The work was supported by the Villum Foundation. The authors acknowledge funding under the Australian Research Council Discovery Project (R.D.T., DP190102659 and DP200100143, J.J.G. DP210102698).

Keywords: electrocatalysis, hydrogen evolution, electrochemical impedance spectroscopy, nanoparticles, ruthenium, solvothermal synthesis

References

[1] A. Hauch, R. Küngas, P. Blennow, A. B. Hansen, J. B. Hansen, B. V. Mathiesen, M. B. Mogensen, *Science* **2020**, *370*, eaba6118.

[2] aY. Zheng, Y. Jiao, A. Vasileff, S. Z. Qiao, *Angew. Chem. Int. Ed.* **2018**, *57*, 7568-7579; bP. Wang, K. Jiang, G. Wang, J. Yao, X. Huang, *Angew. Chem.* **2016**, *128*, 13051-13055.

[3] aZ. W. Seh, J. Kibsgaard, C. F. Dickens, I. Chorkendorff, J. K. Nørskov, T. F. Jaramillo, *Science* **2017**, *355*, eaad4998; bR. Subbaraman, D. Tripkovic, D. Strmcnik, K.-C. Chang, M. Uchimura, A. P. Paulikas, V. Stamenkovic, N. M. Markovic, *Science* **2011**, *334*, 1256-1260.

[4] J. Mao, C.-T. He, J. Pei, W. Chen, D. He, Y. He, Z. Zhuang, C. Chen, Q. Peng, D. Wang, *Nat. Comm.* **2018**, *9*, 1-8.
[5] J. Creus, J. De Tovar, N. Romero, J. García-Antón, K. Philippot, R. Bofill, X. Sala, *ChemSusChem* **2019**, *12*, 2493-2514.
[6] Y. Liu, X. Li, Q. Zhang, W. Li, Y. Xie, H. Liu, L. Shang, Z. Liu, Z. Chen, L. Gu, *Angew. Chem. Int. Ed.* **2020**, *59*, 1718-1726.
[7] aQ. Wang, M. Ming, S. Niu, Y. Zhang, G. Fan, J. S. Hu, *Adv. Energy Mater.* **2018**, *8*, 1801698; bT. Qiu, Z. Liang, W. Guo, S. Gao, C. Qu, H. Tabassum, H. Zhang, B. Zhu, R. Zou, Y. Shao-Horn, *Nano Energy* **2019**, *58*, 1-10; cT. Bhowmik, M. K. Kundu, S. Barman, *ACS Appl. Mater. Interfaces* **2016**, *8*, 28678-28688; dJ. Creus, S. Drouet, S. Suriñach, P. Lecante, V. Collière, R. Poteau, K. Philippot, J. García-Antón, X. Sala, *ACS Catal.* **2018**, *8*, 11094-11102.
[8] C. Xu, M. Ming, Q. Wang, C. Yang, G. Fan, Y. Wang, D. Gao, J. Bi, Y. Zhang, *J. Mater. Chem. A* **2018**, *6*, 14380-14386.
[9] Y. Sugawara, K. Kamata, T. Yamaguchi, *ACS Appl. Energy Mater.* **2019**, *2*, 956-960.
[10] aA. R. Poerwoprajitno, L. Gloag, T. M. Benedetti, S. Cheong, J. Watt, D. L. Huber, J. J. Gooding, R. D. Tilley, *Small* **2019**, *15*, 1804577; bL. Gloag, T. M. Benedetti, S. Cheong, Y. Li, X. H. Chan, L. M. Lacroix, S. L. Chang, R. Arenal, I. Florea, H. Barron, A. S. Barnard, A. M. Henning, C. Zhao, W. Schuhmann, J. J. Gooding, R. D. Tilley, *Angew. Chem. Int. Ed.* **2018**, *57*, 10241-10245.
[11] aK. Byrappa, T. Adschiri, *Prog. in Cryst Growth and Charact. of Mat.* **2007**, *53*, 117-166; bT. Adschiri, Y.-W. Lee, M. Goto, S. Takami, *Green Chem.* **2011**, *13*, 1380-1390; cN. L. N. Broge, F. M. Søndergaard-Pedersen, M. Roelsgaard, X. Hassing-Hansen, B. B. Iversen, *Nanoscale* **2020**, *12*, 8511–8518; dN. L. N. Broge, M. Bondesgaard, F. Søndergaard-Pedersen, M. Roelsgaard, B. B. Iversen, *Angew. Chem. Int. Ed.* **2020**, *59*, 21920 –21924.
[12] J.-L. Mi, Y. Shen, J. Becker, M. Bremholm, B. B. Iversen, *J. Phys. Chem. C* **2014**, *118*, 11104-11110.
[13] aK. Kusada, H. Kobayashi, T. Yamamoto, S. Matsumura, N. Sumi, K. Sato, K. Nagaoka, Y. Kubota, H. Kitagawa, *J. Am. Chem. Soc.* **2013**, *135*, 5493-5496; bT. Zhao, D. Xiao, Y. Chen, X. Tang, M. Gong, S. Deng, X. Liu, J. Ma, X. Zhao, D. Wang, *J. Energy Chem.* **2021**, *61*, 15-22.
[14] aK. Gao, Y. Wang, Z. Wang, Z. Zhu, J. Wang, Z. Luo, C. Zhang, X. Huang, H. Zhang, W. Huang, *Chem. Commun.* **2018**, *54*, 4613-4616; bY. Zheng, Y. Jiao, Y. Zhu, L. H. Li, Y. Han, Y. Chen, M. Jaroniec, S.-Z. Qiao, *J. Am. Chem. Soc.* **2016**, *138*, 16174-16181.
[15] G. Chen, J. Zhang, A. Gupta, F. Rosei, D. Ma, *New J. Chem.* **2014**, *38*, 1827-1833.
[16] aM. Zhao, Y. Xia, *Nat. Rev. Mat.* **2020**, *5*, 440-459; bN. Araki, K. Kusada, S. Yoshioka, T. Sugiyama, T. Ina, H. Kitagawa, *Chem. Lett.* **2019**, *48*, 1062-1064.
[17] C. C. L. McCrory, S. Jung, I. M. Ferrer, S. M. Chatman, J. C. Peters, T. F. Jaramillo, *J. Am. Chem. Soc.* **2015**, *137*, 4347-4357.
[18] aH. Vrubel, T. Moehl, M. Grätzel, X. Hu, *Chem. Commun.* **2013**, *49*, 8985-8987; bS. Anantharaj, S. Ede, K. Karthick, S. S. Sankar, K. Sangeetha, P. Karthik, S. Kundu, *Energy Environ. Sci.* **2018**, *11*, 744-771.
[19] R. K. Shervedani, A. Amini, *Carbon* **2015**, *93*, 762-773.
[20] T. Shinagawa, A. T. Garcia-Esparza, K. Takanabe, *Sci. Rep.* **2015**, *5*, 1-21.

Entry for the Table of Contents

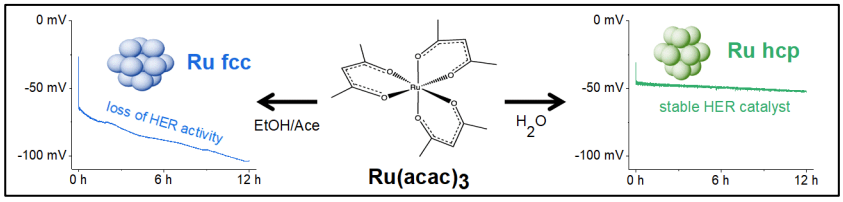

Ru nanoparticles are prepared via solvothermal synthesis with allotropism control over their hcp or fcc structures. Both samples are active catalysts for the hydrogen evolution reaction, but the crystal structure is shown to be important for the stability as only the Ru hcp sample is stable during 12 hour operation.